

ARTICLES

Gas-Phase Stability of Cluster Ions $\text{SF}_m^+ (\text{SF}_6)_n$ with $m = 0-5$ and $n = 1-3$

Kenzo Hiraoka, Akitaka Shimizu, Akihito Minamitsu, Masayuki Nasu, and Susumu Fujimaki

Faculty of Engineering, Yamanashi University, Takeda-4, Kofu 400, Japan

Shinichi Yamabe

Department of Chemistry, Nara University of Education, Takabatake-cho, Nara 630, Japan

The gas-phase stabilities of cluster ions $\text{SF}_m^+ (\text{SF}_6)_n$ with $m = 0-5$ were determined by using a high pressure mass spectrometer. The bond energies of $\text{SF}_m^+ (\text{SF}_6)_1$ were found to be less than 10 kcal/mol and to decrease with $m = 0 \rightarrow 5$. There appear to be rather large gaps in the bond energies between $n = 1$ and 2 for the clusters $\text{SF}_m^+ (\text{SF}_6)_n$ with $m = 0-4$. The structures of SF_5^+ , $\text{SF}_5^+ (\text{SF}_6)_1$, $\text{SF}_3^+ (\text{SF}_6)_1$, and $\text{SF}_5^+ (\text{SF}_6)_1$ were investigated by ab initio molecular orbital calculations. For SF_5^+ , the D_{3h} geometry is found to be most stable and C_{4v} is a transition state of the Berry pseudorotation. For the ion-molecule complexes, the "on-top hat" models were found to be the most stable structures. (*J Am Soc Mass Spectrom* 1995, 6, 1137-1142)

Sulfur hexafluoride has received attention for several decades because of its versatile practical applications. For example, it has been used widely as an efficient insulating gas for high voltage apparatus. Studies of negative ion formation via electron attachment to sulfur hexafluoride molecules in the gas phase have been extensive. Reactions of SF_6 with various positive ions also have been the subject of numerous investigations [1]. Creasey et al. [2] performed detailed measurements of the fragmentation channels and branching ratios for all of the valence states of SF_6^+ . Jiao and Freiser [1] studied reactions of transition-metal ions with SF_6 in the gas phase. They pointed out that the inertness of SF_6 is associated with the protective layer of F atoms that obstructs access to the reactive S center by an attacking species.

The apparently conflicting results for the ionization energy of SF_5 and the standard enthalpy of formation of SF_5^+ have been reported over the past 25 years [3]. Bohme and co-workers [3, 4] investigated ion-molecule reactions of S_2F_{10} with various positive ions and suggested the existence of two isomers for SF_5^+ , that is, a ground-state trigonal bipyramidal (D_{3h}) structure and a less stable square pyramidal structure (C_{4v}). They found that the low energy (D_{3h}) isomer of SF_5^+ reacts with S_2F_{10} to produce $\text{S}_2\text{F}_{11}^+$ and that the high

energy (C_{4v}) isomer reacts with S_2F_{10} to produce SF_3^+ . Cheung et al. [5] performed a theoretical investigation on the geometries of SF_5 and SF_5^+ . They confirmed that the SF_5 (C_{4v}) and SF_5^+ (D_{3h}) structures are true minima, as reported in refs 3 and 4. However, they found that SF_5^+ (C_{4v}) and SF_5 (D_{3h}) structures have imaginary vibrational frequencies, which suggests that these structures are not at local minima. Thus the existence of two isomers for SF_5 and SF_5^+ seems to be still controversial.

Protonated SF_6 (i.e., HSF_6^+) has not been considered to be stable against decomposition to SF_5^+ and HF [6, 7]. Mackay et al. [8] first observed the production of SF_6H^+ as a minor (1%) channel in the reaction of HCO^+ with SF_6 . They predicted the proton affinity (PA) of SF_6 to be 137 ± 1 kcal/mol. Latimer and Smith [9] studied reactions that take place within the core of a free jet flow. They observed the stable HSF_6^+ near 0 K and determined the proton affinity of SF_6 to be 137.9 ± 2.0 kcal/mol, which is in good agreement with the value reported by Mackay et al. [8].

In this work, the clustering reactions of SF_m^+ ($m = 0-5$) with SF_6 were measured via a high pressure mass spectrometer. It was confirmed that SF_6 is a poor nucleophilic reagent toward SF_m^+ ($m = 0-5$) ions and that the interaction between SF_5^+ and SF_6 is exceptionally weak compared to other SF_m^+ ions. Theoretical calculations on the structures of SF^+ , SF_3^+ , SF_5^+ , and their clusters with SF_6 also were performed.

Address reprint requests to Kenzo Hiraoka, Faculty of Engineering, Yamanashi University, Takeda-4, Kofu 400, Japan.

Experimental and Computational

The experiments were performed with a pulsed-electron-beam high pressure mass spectrometer [10, 11]. A copper ion source equipped with a cryocooler (Iwatani Plantech, type-S030) was used to perform low temperature measurements. The N_2 carrier gas was purified by passing it through a liquid N_2 cooled 5-A molecular sieve trap at 3 torr. SF_6 (Iwatani, reagent grade) was introduced into 3 torr of N_2 carrier gas through a flow-controlling stainless steel capillary (0.1 mm \times 1 m). The pressure of SF_6 introduced into the N_2 buffer gas was 0.03–0.8 torr dependent on the experimental conditions. The surface of the ion source was coated with colloidal graphite to prevent charging of the ion source.

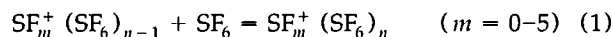
The reagent gas in the reaction chamber was ionized by a pulsed 2-keV electron beam. The produced ions were sampled through a slit made of razor blades (10 μ m \times 1 mm) and were mass-analyzed by a quadrupole mass spectrometer (ULVAC, MSQ-400). The ions were collected in a multichannel analyzer as a function of arrival time after the electron pulse.

Geometries and electronic distributions of SF^+ , SF_3^+ , SF_5^+ , and their SF_6 bound clusters were determined with ab initio molecular orbital calculations. The basis set used is 6-31G^(*), where the polarization function (*) is set on the sulfur atom. This set is needed to describe the hypervalent bond in SF_6 . RHF/6-31G^(*) calculations were carried out for SF_3^+ , SF_5^+ , and their clusters. The UHF/6-31G^(*) calculation was used for SF^+ and $SF^+(SF_6)_1$, because these species are triplet spin states. Spin contaminations were found to be safely small ($\langle S^2 \rangle = 2.02$). For the controversial geometries of SF_5^+ , the following additional calculation was carried out. First, the MP2/6-31G* (used also in [5]) full geometry optimization was made without symmetry constraint. In [4] and [5], C_{4v} and D_{3h} geometries were assumed and the interrelationship between them still was unclear. Second, at the practical C_{4v} geometry, MP2/6-31G* vibrational analysis and subsequent trace of the intrinsic reaction coordinate (IRC) [12] were performed. This IRC calculation gave the overall potential surface of the SF_5^+ isomerization for the first time. All calculations were performed with Gaussian 92 [13] installed on the CONVEX-220 computer (Information Processing Center at Nara University of Education).

Experimental Results

When the reagent gas (N_2 buffer gas that contains a small amount of SF_6) was ionized by a 2-keV electron beam, the positive ions SF_m^+ with $m = 0-5$ were observed as major ions. The relative intensities of S^+ , SF^+ , SF_2^+ , SF_3^+ , SF_4^+ , and SF_5^+ were 0.1, 0.3, 0.4, 2.8, 1.0, and 95.4, respectively, under typical experimental conditions. The SF_6^+ ion was not detected. The absence of SF_6^+ is due to the repulsive nature of the ground state

SF_6^+ , which fragments on a subpicosecond time scale by loss of a fluorine atom to SF_5^+ and F [4]. Under the present experimental conditions, the decay rates of SF_m^+ ions with $m = 0-5$ were found to be slow enough to measure the equilibria for reaction 1:



As an example, the van't Hoff plots for reactions $S_m^+(SF_6)_{n-1} + SF_6 = S_m^+(SF_6)_n$ ($m = 0, 5$) are shown in Figure 1. Thermochemical data for reaction 1 with $m = 0-5$ obtained from the measured van't Hoff plots are summarized in Table 1. In Figure 2, the $-\Delta H_{n-1,n}^\circ$ values for reaction 1 are shown as a function of n .

As shown in Figure 2, the measured $-\Delta H_{n-1,n}^\circ$ values are less than 10 kcal/mol. This indicates that the SF_6 molecule is a rather weak nucleophilic reagent as was pointed out by Rauth et al. [14]. In Figure 2, the $-\Delta H_{0,1}^\circ$ values decrease in the order of $m = 0 \rightarrow 5$. The $-\Delta H_{0,1}^\circ$ values for $m = 0, 1$ and $m = 2, 3, 4$ are close to each other whereas the $-\Delta H_{0,1}^\circ$ value with $m = 5$ is much smaller. This suggests that the bonding in the clusters $SF_m^+(SF_6)_1$ with $m = 0, 1$ and $m = 2-4$ is similar. The smallest bond energy for $SF_5^+(SF_6)_1$ may be due to the well-dispersed positive charge in the SF_5^+ cation with a trigonal bipyramidal structure.

In Figure 2, a sudden drop appears in $-\Delta H_{n-1,n}^\circ$ between $n = 1$ and 2 for $m = 0-4$. This n dependence indicates that the $n = 1$ clusters are relatively more stable than the $n = 2$ clusters for $SF_m^+(SF_6)_n$ with $m = 0-4$. This may suggest a slight participation of a

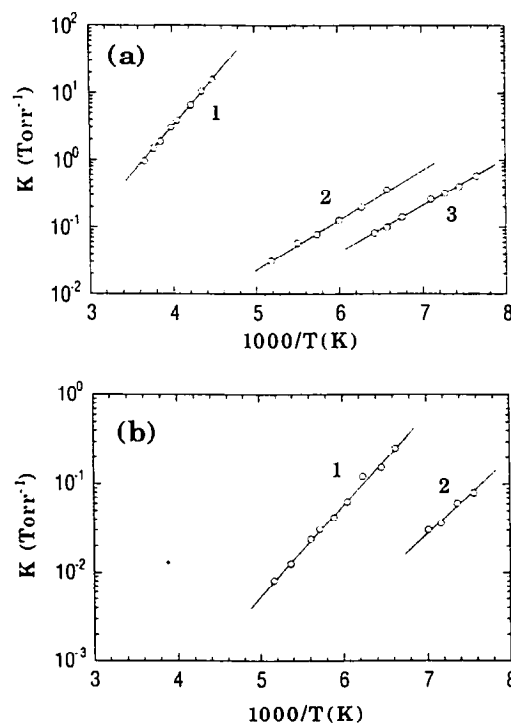


Figure 1. van't Hoff plots of the gas-phase clustering reaction, (a) $S^+(SF_6)_{n-1} + SF_6 = S^+(SF_6)_n$ and (b) $SF_5^+(SF_6)_{n-1} + SF_6 = SF_5^+(SF_6)_n$. Integer numbers in the figure represent values of n .

Table 1. Experimental thermochemical data, $\Delta H_{n-1,n}^\circ$ (kcal/mol) and $\Delta S_{n-1,n}^\circ$ (cal/mol K) (standard state, 1 atm), for gas-phase clustering reactions, $SF_m^+ (SF_6)_{n-1} + SF_6 = SF_m^+ (SF_6)_n$ for $m = 0-5^a$

$n-1, n$	$S^+ (SF_6)_{n-1, n}$		$SF^+ (SF_6)_{n-1, n}$		$SF_2^+ (SF_6)_{n-1, n}$		$SF_3^+ (SF_6)_{n-1, n}$		$SF_4^+ (SF_6)_{n-1, n}$		$SF_5^+ (SF_6)_{n-1, n}$	
	$-\Delta H^\circ$	$-\Delta S^\circ$	$-\Delta H^\circ$	$-\Delta S^\circ$	$-\Delta H^\circ$	$-\Delta S^\circ$	$-\Delta H^\circ$	$-\Delta S^\circ$	$-\Delta H^\circ$	$-\Delta S^\circ$	$-\Delta H^\circ$	$-\Delta S^\circ$
0, 1	9.4	21	9.1	20	7.8	18	7.4	25	7.2	23	4.7	21
			[7.07] ^c				[7.63] ^c				[5.49] ^c	
1, 2	3.4	11	3.8	16	5.0	22	4.5	19	4.6	14	3.6	19
2, 3	3.0	11	3.7	17	4.2	20	4.0	(19) ^b				

^aExperimental errors for $\Delta H_{0,1}^\circ$ and $\Delta S_{0,1}^\circ$ are 0.5 kcal/mol and 2 cal/mol K, and those for $\Delta H_{n-1,n}^\circ$ and $\Delta S_{n-1,n}^\circ$ with $n \geq 2$ are 0.2 kcal/mol and 2 cal/mol K, respectively.

^bEntropy value assumed.

^cValues in square brackets denote MP2/6-31G**/HF/6-31G(1') theoretical binding energies, ΔE_s .

covalent bond in these $n = 1$ clusters. However, the ground electronic spin states of S^+ and SF^+ are quartet and triplet, respectively, and the spin conservation in the formation of cluster ions ($n = 1$) with some covalency may be highly endothermic for these cations. Thus, the observed sudden drop in the $-\Delta H_{n-1,n}^\circ$ between $n = 1 \rightarrow 2$ for $SF_m^+ (SF_6)_n$ ($m = 0-4$) may be due to mainly the steric effect (e.g., exchange repulsion between ligand SF_6 molecules) in the cluster ions.

In Table 1, a drastic decrease in $-\Delta S_{n-1,n}^\circ$ is observed with $n = 1 \rightarrow 2$ for $S^+ (SF_6)_n$. This indicates that the freedom of motion for $n \geq 2$ SF_6 ligands is much less restricted than the $n = 1$ SF_6 . It is likely that the $S^+ (SF_6)_1$ forms the core in the larger cluster ions, that is, $[S^+ (SF_6)_1] (SF_6)_{n-1}$.

Computational Results

In the previous section, three groups of the binding energies ($m = 0, 1, m = 2, 3, 4$, and $m = 5$) have been recognized. Geometries and electronic distributions of $m = 1, 3, 5$ are considered in respective groups. This selection comes from the fact that $S^+ (SF_6)_1$, $SF_2^+ (SF_6)_1$, and $SF_4^+ (SF_6)_1$ require a more accurate (multiconfigurational) wavefunction than the Hartree-Fock and their geometry optimization is beyond the present computational facility.

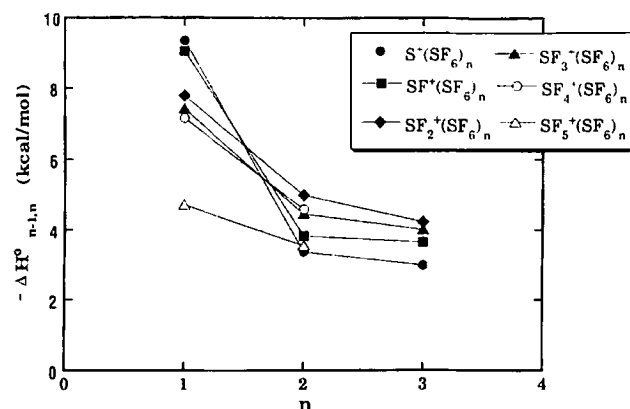
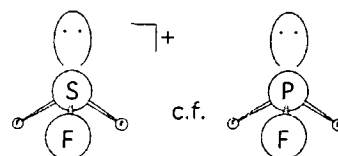
**Figure 2.** The n dependence of the $-\Delta H_{n-1,n}^\circ$ values of clustering reaction 1, $SF_m^+ (SF_6)_{n-1} + SF_6 = SF_m^+ (SF_6)_n$ with $m = 0-5$.

Figure 3 shows fragments SF_6 , SF^+ , and SF_3^+ before cluster formation. The SF_6 molecule is confirmed to be of O_h point group, and the S atom is quite cationic (+1.93). SF^+ is valence isoelectronic with S_2 and O_2 , and it is a triplet spin state. The sulfur atom in SF^+ is quite cationic (+1.20). SF_3^+ is a nonplanar molecule as is expected from the Walsh rule [15] for AB_3 -type molecules. Although the sulfur atom in SF_3^+ is very cationic (+1.58), there is a lone-pair orbital along the principal axis.



Therefore, the principal-axis coordination is thought to be unfavorable due to exchange repulsion.

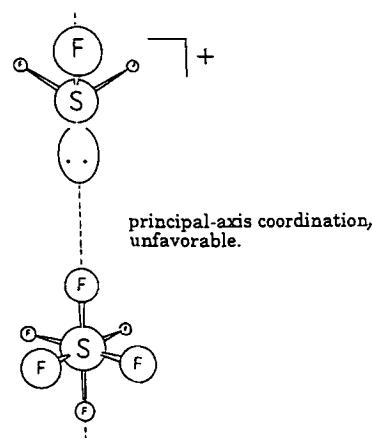


Figure 4 shows geometries for SF_5^+ along the isomerization path. The C_{4v} geometry is confirmed to be a transition state [5] with the sole imaginary frequency $\nu = 140.1 \text{ i cm}^{-1}$. Next, the reaction-coordinate vector that corresponds to the frequency is traced along the reaction path (IRC) [12]. Two energy-minimum points ($S = -5.5$ and $+5.5$) are found to be D_{3h} isomers. Thus, the C_{4v} geometry is of a transition state for the Berry pseudorotation [16] between two D_{3h} geometries.

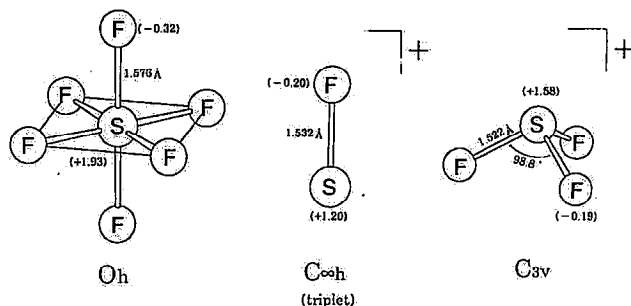
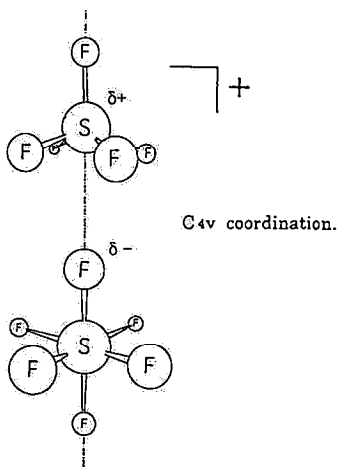


Figure 3. Geometries of SF_6 , SF_5^+ , and SF_3^+ fully optimized with RHF/6-31G*. Values in parentheses denote atomic charges (positive, cationic).

tries. A similar pseudorotation has been found in SiF_4^- [17], which is isoelectronic with SF_5^+ . Thus, the pseudorotation is a common characteristic in SiX_5^- , PX_5 , and SX_5^+ ($\text{X} = \text{F}$ and Cl).

The C_{4v} SF_5^+ might give an effective Coulombic attraction along the principal axis.



Berry Pseudorotation of SF_5^+ .

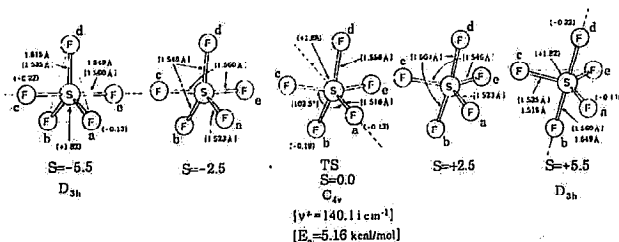


Figure 4. Interrelationship between C_{4v} and D_{3h} geometries of SF_5^+ along the intrinsic reaction coordinate (IRC) [12] of the isomerization. From the transition state (TS, the C_{4v} symmetry), two ways of the distortion lead to D_{3h} stable isomers. Bracket values are of MP2/6-31G* for the IRC calculation. Interrupted lines stand for principal axes of C_{4v} and D_{3h} point groups. S values denote reaction coordinates (Bohr $\text{u}^{1/2}$). ν and E_a of C_{4v} are the sole imaginary frequency and the activation energy of MP2/6-31G*, respectively.

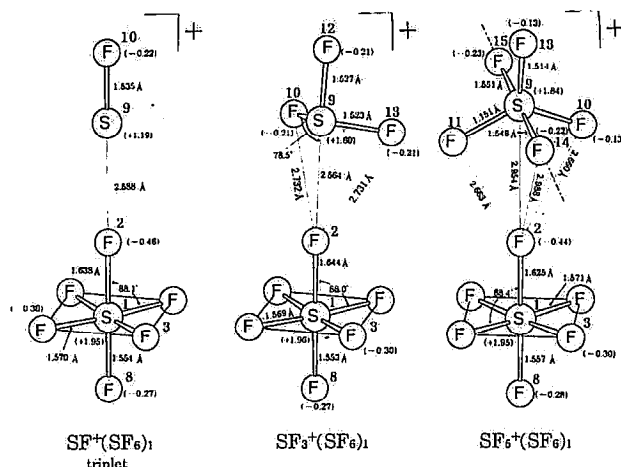
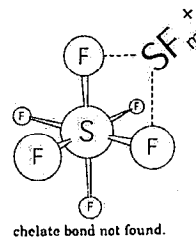


Figure 5. Geometries of three $n = 1$ clusters. For $\text{SF}_3^+(\text{SF}_6)_1$, the principal axis of the SF_3^+ moiety is shown by an interrupted line.

It is of structural interest to examine whether the C_{4v} coordination is favored in spite of the $E_a = 5.16$ kcal/mol instability shown in Figure 4.

Figure 5 exhibits optimized structures of three $n = 1$ clusters. As shown in the figure, the top-hat coordinations are found to be most stable. No chelate-bond-type coordinations are found.



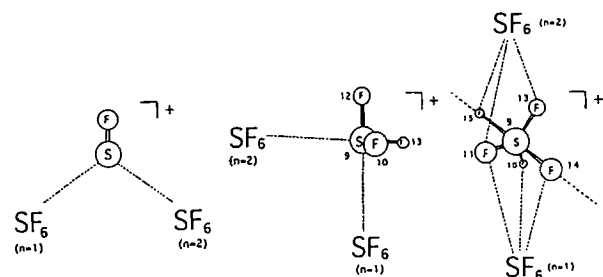
In $\text{SF}^+(\text{SF}_6)_1$, the intermolecular $\text{S}^{\delta+} \cdots \text{F}^{\delta-}$ distance is large ($= 2.59$ Å), which corresponds to the small $-\Delta H_{0,1}^\circ = 9.1$ kcal/mol in Table 1. The $\text{S}-\text{F}$ bond length ($= 1.535$ Å) in the SF^+ moiety is almost the same as that in the free SF^+ ($= 1.532$ Å in Figure 3). On the other hand, the SF_6 geometry is somewhat distorted due to cluster formation. Noticeably, the S^1-F^2 bond is elongated (1.576 Å in $\text{SF}_6 \rightarrow 1.638$ Å in the cluster). Along with this elongation, the F^2 atom becomes more anionic (-0.46) than that (-0.32) in the free SF_6 . Because the $\text{SF}_6 \rightarrow \text{SF}^+$ charge shift is small ($0.03e$ in $\text{SF}_6 \rightarrow \text{SF}^+$ and $\text{SF}_6 \rightarrow \text{SF}_3^+$, and $0.02e$ in $\text{SF}_6 \rightarrow \text{SF}_5^+$; present work), the SF_6 distortion is ascribed to the polarization.

$\text{SF}_3^+(\text{SF}_6)_1$ has the structure of the S_N2 back-side attack along a $\text{S}-\text{F}$ bond in SF_3^+ . The principal-axis coordination is not obtained as is predicted. $\text{F}^2 \cdots \text{F}^{10}$

and $F^2 \cdots F^{13}$ distances are 2.73 Å. Exchange repulsion of these pairs blocks the further $S^9 \cdots F^2$ approach. The geometry of SF_6 is distorted slightly as in SF_5^+ (SF_6)₁.

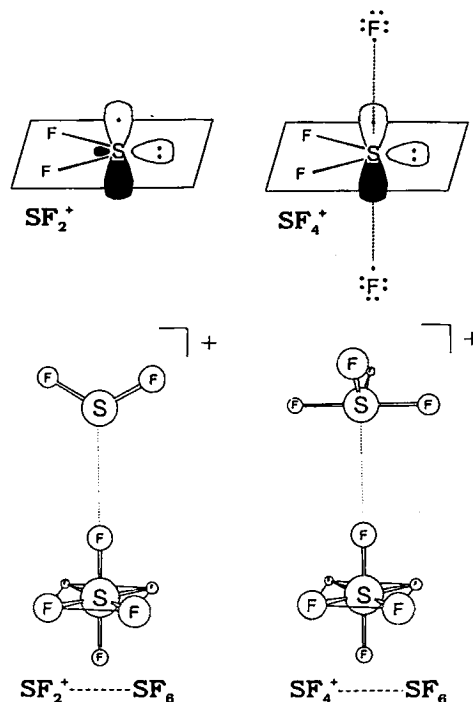
In SF_5^+ (SF_6)₁, the D_{3h} SF_5^+ is retained and is not isomerized to the C_{4v} structure, although the latter is a better electrophile toward SF_6 . F^{10} , F^{11} , and F^{14} in SF_5^+ block the $S^9 \cdots F^2$ attraction, which leads to its large distance (= 2.95 Å) and consequently to the small binding energy (= 4.7 kcal/mol in Table 1).

The geometries of the SF_6 adducts with $n = 2$ may be estimated in view of the three $n = 1$ geometries shown in Figure 5. In SF^+ (SF_6)₁, the principal-axis coordination has been obtained. The second SF_6 is obligated to be linked with SF^+ as shown in succeeding text. This drastic change of the sterically crowded coordination corresponds to the large fall-off of $-\Delta H_{n-1,n}^\circ$ (9.1 kcal/mol of $n = 1 \rightarrow 3.8$ kcal/mol of $n = 2$) in Table 1. In SF_3^+ (SF_6)₂, the second SF_6 is directed to another S—F (say, $S^9 - F^{13}$) bond. In SF_5^+ (SF_6)₂, the second SF_6 is attached to the (F^{13}, F^{15}, F^{11}) or (F^{13}, F^{15}, F^{10}) triangle of SF_5^+ .



The smallest fall-off in $-\Delta H_{n-1,n}^\circ$ (4.7 kcal/mol for $n = 1 \rightarrow 3.5$ kcal/mol for $n = 2$) has been obtained for SF_5^+ (SF_6)_n in Table 1. This comes from the almost undisturbed D_{3h} SF_5^+ , where the coordination of SF_6 ligands to the cation center (the sulfur atom) is blocked by two equatorial and one apical fluorine atoms. As an indication of structural analyses, $n = 1$ binding energies are controlled by the extent of the $F \cdots F$ exchange repulsion. The bonding is mainly electrostatic with slight participation of a covalent bond (i.e., the bonding density 0.02 between F^2 and S^9 atoms in three clusters). The $n = 1 \rightarrow 2$ fall-off in energies is determined by the extent of $SF_6 \cdots SF_6$ repulsion. The computed binding energies (ΔE s) given in square brackets in Table 1 for SF_3^+ (SF_6)₁ and SF_5^+ (SF_6)₁ are in good agreement with $\Delta H_{0,1}^\circ$ s. However, $-\Delta E$ of SF^+ (SF_6)₁ (7.07 kcal/mol) is underestimated. The UHF triplet calculation has some problems.

Although SF_m^+ (SF_6)₁ clusters ($m = 0, 2, 4$) have not been dealt with theoretically, their geometries can be predicted. $S^+ \cdots SF_6$ would be of principal-axis coordination with C_{4v} symmetry. SF_2^+ is a π radical, and SF_4^+ is composed of SF_2^+ and two fluorine atoms attached perpendicularly to the radical center S^+ .



SF_2^+ and SF_4^+ would be coordinated by the electrostatic force to SF_6 along the SF_6 principal axis with C_{2v} symmetry. The $SF_2^+ \cdots SF_6$ geometry is based on our rough calculations. Although the $SF_4^+ \cdots SF_6$ C_{2v} geometry is reasonable, the charge-transfer π radical on-top coordination in $SF_2^+ \cdots SF_6$ also might be likely. In any event, the principal-axis coordination of the sulfur atom in SF_m^+ is a uniform pattern in $SF_m^+ \cdots SF_6$ geometries.

Concluding Remarks

In this work, clustering reactions between sulfur hexafluoride and its fragment cations have been investigated. All SF_m^+ (SF_6)₁ clusters have small binding energies (< 10 kcal/mol) and they involve top-hat coordinations. The charge transfer $SF_6 \rightarrow SF_m^+$ is small, but the polarization in SF_6 is appreciable. The controversial geometries of SF_5^+ have been examined, and the Berry pseudorotation of $C_{4v}(TS) \rightarrow D_{3h}$ isomers has been obtained along the intrinsic reaction coordinate. The D_{3h} geometry is almost retained in SF_5^+ (SF_6)₁, which leads to the smallest binding energy among SF_m^+ (SF_6)₁. The inertness of SF_6 against SF_m^+ cations is recognized in two aspects: One is the intrinsically weak intermolecular bond shown in SF^+ (SF_6)₁; the other is the $F \cdots F$ exchange block shown in SF_3^+ (SF_6)₁ and SF_5^+ (SF_6)₁.

Acknowledgments

We express our appreciation for the financial support of the Morino Foundation for Molecular Science and the grand-in-aid for scientific research from the Ministry of Education, Science, and Culture, Japan.

References

1. Jiao, C. Q.; Freiser, B. S. *J. Am. Chem. Soc.* **1993**, *115*, 6268.
2. Creasey, J. C.; Jones, H. M.; Tuckett, R. P.; Hatherly, P. A.; Codling, K.; Powis, I. *Chem. Phys.* **1993**, *174*, 441.
3. Becker, H.; Hrusak, J.; Schwarz, H.; Bohme, D. K. *J. Chem. Phys.* **1994**, *100*, 1759.
4. Javahery, G.; Becker, H.; Korobov, M. V.; Farber, M.; Cooper, D.; Bohme, D. K. *Int. J. Mass Spectrom. Ion Processes* **1994**, *133*, 73.
5. Cheung, Y-S.; Li, W-K.; Chiu, S-W.; Ng, C. Y. *J. Chem. Phys.* **1994**, *101*, 3412.
6. Tichy, M.; Javahery, G.; Twiddy, N. D.; Ferguson, E. E. *Int. J. Mass Spectrom. Ion Processes* **1987**, *79*, 231.
7. Adams, N. G.; Smith, D.; Tichy, M.; Javahery, G.; Twiddy, N. D.; Ferguson, E. E. *J. Chem. Phys.* **1989**, *91*, 4037.
8. Mackay, G. I.; Schiff, H. I.; Bohme, D. K. *Int. J. Mass Spectrom. Ion Processes* **1992**, *117*, 387.
9. Latimer, D. R.; Smith, M. A. *J. Chem. Phys.* **1994**, *101*, 3410.
10. Kebarle, P. In *Techniques for the Study of Ion-Molecule Reactions*; Farrar, J. M.; Saunders, W. S., Eds.; Wiley: New York, 1971; p 221.
11. Hiraoka, K.; Yamabe, S. In *Dynamics of Excited Molecules*; Kuchitsu, K., Ed.; Elsevier: Amsterdam, 1994; p 399.
12. (a) Fukui, K. *J. Phys. Chem.* **1970**, *74*, 4161; (b) Gonzalez, C.; Schlegel, H. B. *J. Phys. Chem.* **1990**, *94*, 5523.
13. Frisch, M. J.; Head-Gordon, M.; Gill, P. M. E.; Wong, M. W.; Foreman, J. B.; Johnson, B. G.; Schlegel, H. B.; Robb, M. A.; Replogle, E. S.; Gomperts, R.; Andres, J. L.; Raghavachari, K.; Binkley, J. S.; Gonzalez, C.; Martin, R. L.; Fox, D. J.; DeFrees, D. J.; Baker, J.; Stewart, J. J. P.; Pople, J. Gaussian 92, Revision C, Gaussian, Inc., Pittsburgh, PA, 1992.
14. Rauth, T.; Echt, O.; Mark, T. D. *Chem. Phys. Lett.* **1993**, *201*, 345.
15. Walsh, A. D. *J. Chem. Soc.* **1953**, 2260.
16. (a) Berry, R. S. *J. Chem. Phys.* **1960**, *32*, 933; (b) Mislou, K. *Acc. Chem. Res.* **1970**, *3*, 321.
17. Windas, T. L.; Gordon, M. S.; Davis, L. P.; Burggraf, L. W. *J. Am. Chem. Soc.* **1994**, *116*, 3568.